Transactions of the 15th International Conference on
Structural Mechanics in Reactor Technology (SMiRT-15)
Seoul, Korea, August 15-20, 1999

Circumferential Fatigue Crack Growth and Crack Opening Behavior in Pipes Subjected to Bending Moment

Yeon-Sik Yoo and Kotoji Ando

Yokohama National University, Japan

ABSTRACT

A series of fatigue tests has been carried out at room temperature on carbon steel pipe, which has an inner surface crack. The main results obtained in this study were as follows: (1) Before crack penetration, fatigue crack growth behavior such as aspect ratios and leak life were evaluated by using the proposed plate model and Newman-Raju's formula. (2) After crack penetration, a new formula to evaluate K was proposed. For a complex crack after through wall, fatigue crack growth behavior, fatigue life and crack opening displacement were evaluated quantitatively by using the new formula and the pipe model proposed in this study.

INTRODUCTION

The LBB(Leak Before Break) design used for energy-related plants such as nuclear piping systems and high pressure vessels has recently been attracting much interest from a safety and economic point of view. The LBB concept is a design philosophy to guarantee that the unstable fracture does not occur before crack penetrates the wall thickness and even after the complete penetration, the unstable fracture does not occur for a certain period. Especially, studies about the unstable fracture due to a crack in structure have been performed on various aspects[1,2]. The present authors have reported an systematic investigation on the LBB condition, the fatigue crack growth and crack opening behavior of a plate under fatigue stress[3]. Studies of the crack propagation behavior and the crack opening displacement on a complex through crack after crack penetration in pipe, however, are relatively rare.

To that purpose, the present authors have proposed a simplified evaluation model for determining the stress intensity factor after crack penetration in pipe[6,7]. It was found that the crack propagation characteristics, the crack shape changes and the crack opening displacement after crack penetration in pipe with an inner surface crack could be evaluated quantitatively by using the proposed formula and pipe model in this study.

EVALUATION OF STRESS INTENSITY FACTOR

The stress intensity factor before crack penetration was estimated by using the plate model and Newman-Raju's formula[4]. The plate model proposed was shown in Fig.1. In this plate model, following assumptions were made: plate width(2W) corresponds to the outer perimeter of pipe($2\pi R_S$), plate thickness is equal to pipe thickness(t). Crack depth is a, inner surface crack length is $2C_B$ and the plate was subjected to a tensile and bending stress component considered from the actual bending stress(σ_B).

In order to evaluate crack growth behavior after crack penetration, following pipe model was considered. On the basis of this pipe model, four assumptions were made for deriving the stress intensity factor.

1. The crack opening displacement at the center of the crack after penetration (on the line X-X' in Fig.2) is assumed to be the same on the outer surface and inner surface.

2. After crack penetration, a crack is located symmetrically around the maximum tensile stress, stress is calculated elastically and one half of the crack angle, θ_M, on the midsection is given by the following equation.

$$\theta_M = \frac{(\theta_S + \theta_B)}{2} \tag{1}$$

3. The crack opening displacement $\delta(\theta_M)$ at the center of the wall thickness (on the line X-X' in Fig.2) is assumed to be the same as the crack opening displacement at the center of a simple through wall crack with a crack angle $2\theta_M$ in a pipe.

Hence, $\delta(\theta_M)$ can be expressed as follows[5]:

$$\delta(\theta_M) = 4\sigma_B \cdot \{R_S - (t/2)\}\theta_M \cdot V_b / E \tag{2}$$

where,

$$V_b = 1 + A\left\{6.071(\theta_M/\pi)^{1.5} + 24.15(\theta_M/\pi)^{2.94}\right\}$$
$$A = \left[0.125\{(R_s - (t/2))/t\} - 0.25\right]^{0.25}$$
$$(valid\ range: 5 \le \{R_S - (t/2)\}/t \le 10)$$

4. The stress intensity factors K_S and K_B at points S and B(see Fig.2) after crack penetration are assumed to be equal to the stress intensity factors in simple through wall cracks with a crack angle $2\theta_S$ or $2\theta_B$ respectively. The crack opening displacement at the center is, moreover, exposed to the elastic bending stress corresponding to $\delta(\theta_M)$.

These four assumptions make it possible to express the stress intensity factors for a complex through wall crack at points S and B in Fig.2 by using the K formula for a simple through wall crack[5].

$$K_S = K(\theta_S) = \delta(\theta_M)/\delta(\theta_S) \cdot \sigma_B \cdot [\pi \cdot R_S \cdot \theta_S]^{0.5} \cdot F_b(\theta_S) \tag{3}$$
$$K_B = K(\theta_B) = \delta(\theta_M)/\delta(\theta_B) \cdot \sigma_B \cdot [\pi \cdot (R_S - t) \cdot \theta_B]^{0.5} \cdot F_b(\theta_B) \tag{4}$$

where,

$$F_b(\theta_S) = 1 + A\left\{4.5976(\theta_S / \pi)^{1.5} + 2.6422(\theta_S / \pi)^{4.24}\right\}$$
$$F_b(\theta_B) = 1 + A\left\{4.5976(\theta_B / \pi)^{1.5} + 2.6422(\theta_B / \pi)^{4.24}\right\}$$

$\delta(\theta_S)$ or $\delta(\theta_B)$ can be written by substituting θ_S or θ_B for θ_M in formula(2), and $V_b(\theta_S)$ or $V_b(\theta_B)$by substituting θ_S or θ_B for θ_M in $V_b(\theta_M)$.

MATERIAL AND TESTING PROCEDURE

The pipe used in this study was carbon steel of STS370, which had the following mechanical properties: yield stress 227MPa, tensile strength 406MPa and percentage of elongation 25.3%. The specimen geometry, the stress conditions and so on was shown in Table 1. The initial notch of length $2C_{B0}$ and depth a_0 was located on the inner surface of the specimens using an electric discharge machine or saw. The specification of fatigue test was four point bending test system which has an outer span of 1000mm and an inner span of 245mm The fatigue tests were carried out under load control at room temperature using an electrohydraulic fatigue test machine with capacity of 0.245MN. The test conditions were as follows: sine wave loading, stress ratio R=0.1, and frequency 1～5Hz. Crack propagation to the circumferential and depth direction were measured by a stereomicroscope and beach marks. A clip gauge measured crack opening displacement after crack penetration.

TEST RESULTS AND CONSIDERATIONS

Crack Growth Behavior before Crack Penetration

Photographs of the fatigue fracture surfaces obtained from experiment are illustrated in Fig.3. Fig.3 shows the results obtained from the specimens with an initial inner surface crack subjected to elastic or elastic-plastic bending stress. A comparison between the measured aspect ratios from the beach marks of Fig.3 and the calculated ones from Newman-Raju's formula and the proposed plate model is shown in Fig.4. From this figure, the following fatigue crack growth characteristics can be pointed out:

(a) The calculated aspect ratios show a good agreement with the experimental ones regardless of initial aspect ratio, bending stress level and wall thickness.

(b) When initial aspect ratio is small, it increases with crack growth. However, in the case of large initial aspect ratio, it decreases with crack growth. Moreover, in the case of moderate initial aspect ratio, it shows a convex curve and a maximum value on the way.

The fatigue crack penetration behavior obtained from experiment was also examined in this study. As a result of that, a correlation between the normalized half crack length at crack penetration(C_{BL}) and the normalized initial half crack length(C_{B0}) is shown in Fig.5. From this figure, the following characteristic can be pointed out: When C_{B0}/t is lower than about 1.3, C_{BL}/t shows almost constant value of 1.3. However, as C_{B0}/t is greater than about 1.3, C_{BL}/t and C_{B0}/t indicate almost same value regardless of the bending stress level and wall thickness. Therefore, from above results, it is possible to assume the crack length at crack penetration if an initial crack length and a wall thickness are known.

Crack Opening and Crack Growth Behavior after Crack Penetration

Fatigue crack growth and crack opening behavior after crack penetration is also important factors in the viewpoint of the structure integrity and the proper design of piping system. Crack opening displacement was measured by a clip gauge at maximum tensile stress point and calculated by formula(2). Fig.6 shows a comparison between the experimental crack opening displacement per load($\delta(\theta_M)/P$) as function of one half of the midsection crack angle(θ_M) and the calculated ones. Although a little scattering is presented in experimental data before θ_S becomes to be equal to θ_B, a quite good agreement between the experimental and the calculated ones is generally represented regardless of bending stress level and crack length at crack penetration. These results of Fig.6 make it possible to evaluate the stress intensity factor quantitatively for a complex through wall crack.

Fig.7 shows a correlation between the normalized outer half crack angle(θ_S/π) and the normalized inner half crack angle(θ_B/π). From this figure, the following characteristic can be pointed out: Until an outer surface crack angle(θ_S) catches up with an inner surface crack angle(θ_B) immediately after crack penetration, θ_S grows rapidly. Then, after θ_S becomes to be equal to θ_B, fatigue crack grows with maintaining same crack angle in the outer and inner surface, which means the crack growth behavior of a simple through crack. In Fig.7, a comparison between the experimental crack angle ratios and the calculated ones from the proposed formula(3),(4) and pipe model shows a good agreement despite of bending stress level and crack length at crack penetration.

Fatigue Crack Growth Rate versus Stress Intensity Factor Range

Fatigue crack growth rate versus stress intensity factor range obtained from specimens with an inner surface crack is illustrated in Fig.8. On the calculation of fatigue crack growth rate, the number of cycles prior to the first beach mark was neglected in order to eliminate the influence of crack initiation life. Before crack penetration, the stress intensity factor range(ΔK) was evaluated by using Newman-Raju's formula and the proposed plate model. After crack penetration, the stress intensity factor range was evaluated by using the proposed formula and pipe model. The data of Fig.8 include four kinds of crack growth rates as following: ones to the depth direction(da/dN)and ones to the inner surface(dC_B/dN) before crack penetration, ones to the outer surface(dC_S/dN) and ones to the inner surface(dC_B/dN) after crack penetration. From these figures, a correlation between the four kinds of crack growth rates and the stress intensity factor range can be expressed as following equation regardless of initial crack shape and bending stress level.

$$da/dN(mm/cycle) = 3.20\times10^{10}(\Delta K)^{3.72}\left(MPa\sqrt{m}\right) \quad (5)$$

Fatigue Life

Fatigue life at and after crack penetration was evaluated in this study. A comparison between the experimental and the calculated values of leak life(N_L) at crack penetration is illustrated in Fig.9. The calculation of leak life was done by using the above equation(5), Newman-Raju's formula and the proposed plate model. The results of the calculated leak life show an excellent agreement with the experimental ones regardless of initial crack location and bending stress level.

After crack penetration, a comparison between the calculated and the experimental fatigue crack

growth behavior after crack penetration is shown in Fig.10. The calculation was obtained from the above equation(5), the formula(3), (4) and the pipe model proposed in this study. Although a little scattering between the experimental and the calculated ones was shown in this figure, the calculated values represent a sufficient characteristic of the actual fatigue crack growth behavior.

A comparison between the calculated and the experimental values of N_{40} is illustrated in Fig.11. At this, N_{40} means the number of cycles when C_3 reaches 40mm after crack penetration. Although the experimental scattering is shown in this figure, the calculated values of N_{40} from the above equation(5), the formula(3), (4) and the pipe model proposed in this study, on the whole, show a good agreement with the experimental ones regardless of bending stress level and crack length at crack penetration.

CONCLUSION

A series of fatigue tests has been carried out at room temperature in air on carbon steel pipes, which have an initial inner surface crack. Special attention was paid to fatigue crack growth and penetration behavior. The main results obtained in this study were as follows:

(1) A new formula was proposed for evaluating K for complex cracks after crack penetration in pipe subjected to bending moment.

(2) Before crack penetration, fatigue crack growth behavior such as the change of crack shape and leak life were evaluated successfully by using Newman-Raju's formula and the proposed plate model.

(3) After crack penetration, fatigue crack growth behavior such as the change of crack shape, fatigue life and crack opening displacement were evaluated quantitatively for complex cracks by using the equation and pipe model proposed in this study.

REFERENCES

1. Hasegawa, K., Sakata, S., Simizu, T. and Shida, S., "Prediction of Fracture Tolerances for Stainless Steel Pipes with Circumferential Cracks," ASME Int. J. Press. Ves. and Piping. 95, 1983, pp. 65-78.
2. Shibata, K., Yokoyama, N., Ohba, T., Kawamura, T. and Miyazono, S., "Growth Evaluation of Fatigue Cracks from Multiple Surface Flaws(II)," J. Atomic Energy Soc. Jpn 28, 1986, pp. 258-265(in Japanese).
3. Nam, K. W., Ando, K., Ogura, N. and Matsui, K., "Fatigue Life and Penetration Behavior of Surface-Cracked Plate under Combined Tensile and Bending Stress," Fatigue Fract. Engng Mater. Struct.17, 1994, pp. 873-880.
4. Newman, J. C. Jr. and Raju, I, S., "An Empirical Stress Intensity Factor Equation for the Surface Crack," Engng. Fract. Mech. 15, 1981, pp. 185-192.
5. Zahoor, A., Ductile Fracture Handbook. 3, Novetech Corporation and Electric Power Research Institute, 1989.
6. Ahn, S. H., Hidaka, A. and Ando, K., "Fatigue Crack Growth and Penetration Behavior in Pipe Subjected to Bending Load," Structural Mechanics in Reactor Technology. 4, pp. 113-120, 1997.
7. Yoo, Y. S., Ahn, S. H. and Ando, K., "Fatigue Crack Growth and Penetration Behavior in Pipes Subjected to Bending Moment," ASME. PVP-Vol.371, pp. 63-70, San-Diego U.S., Aug. 1998.

Table 1 Specimen geometry, stress condition and fatigue life

No.	Specimen Geometry					Stress Condition		Fatigue Life	
	$2C_{B0}$ (mm)	a_0 (mm)	R_S (mm)	t (mm)	$2\theta_0$† (deg.)	σ_{max} (MPa)	σ_{min} (MPa)	N_L‡ (cycle)	N_F‡ (cycle)
TB-1	44.5	4.5	51.0	8.1	59.4	200.0	20.0	12407	21558
TB-2	12.0	3.0	51.0	8.1	16.0	210.0	21.0	169750	197856
TB-3	10.0	5.0	51.0	8.1	13.4	325.0	32.5	11200	17500
TB-4	36.5	3.0	51.0	8.1	48.8	200.0	20.0	72910	86260
TB-5	12.0	6.0	51.0	12.7	18.0	220.0	22.0	222920	245800
TB-6	12.0	3.0	51.0	12.7	18.0	261.0	26.1	287500	301400

† $2\theta_0$: Initial Crack Angle ‡ N_L : Number of Cycles to Leak, N_F : Number of Cycles to Fracture

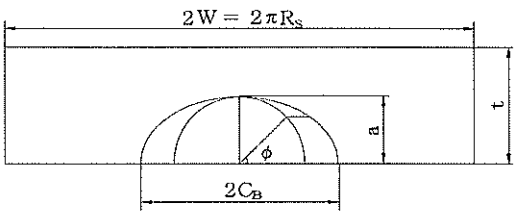

Fig.1 Model to evaluate stress intensity factor before crack penetration

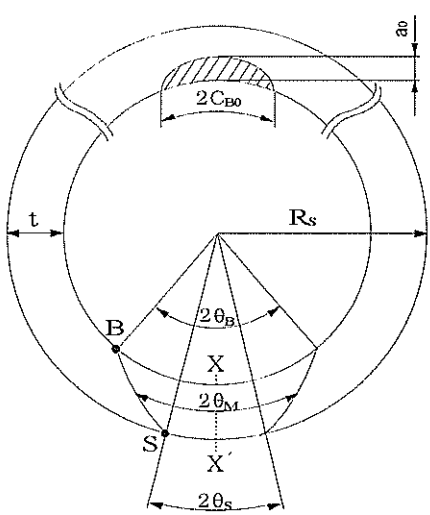

Fig.2 Model to evaluate stress intensity factor after crack penetration

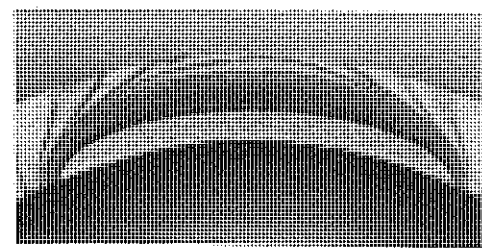

(a) TB-4 ($2C_{B0}$ = 36.5 mm, a_0 = 3.0 mm)

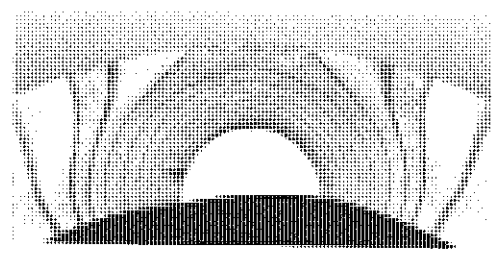

(b) TB-5 ($2C_{B0}$ = 12.0 mm, a_0 = 6.0 mm)

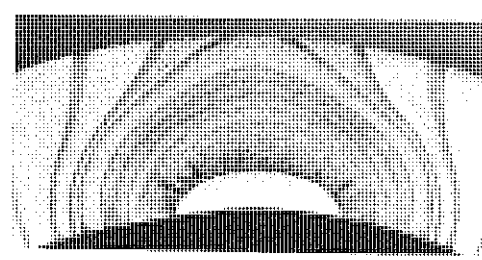

(c) TB-6 ($2C_{B0}$ = 12.0 mm, a_0 = 3.0 mm)

Fig.3 Photographs of fatigue fracture surface

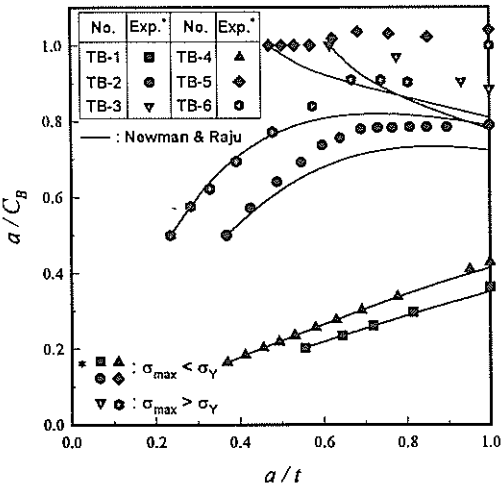

Fig.4 Aspect ratios(a/C_B) versus a/t

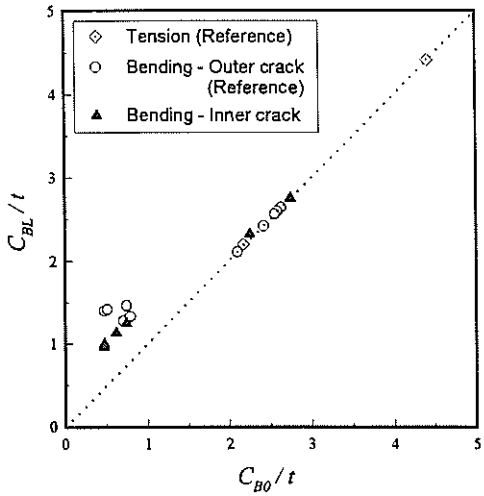

Fig.5 Correlation between the normalized half crack length at penetration and the normalized initial half crack length

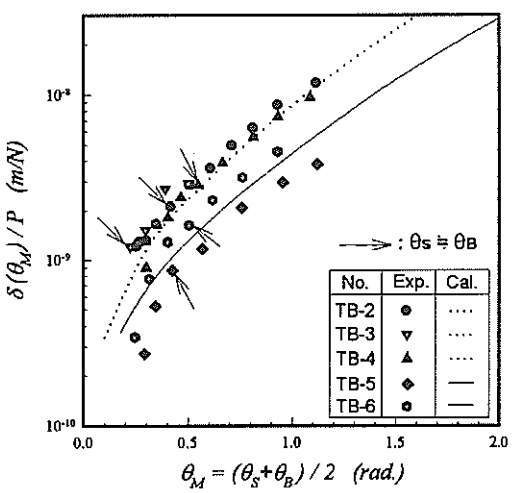

Fig.6 Comparison between the calculated and the experimental COD after penetration

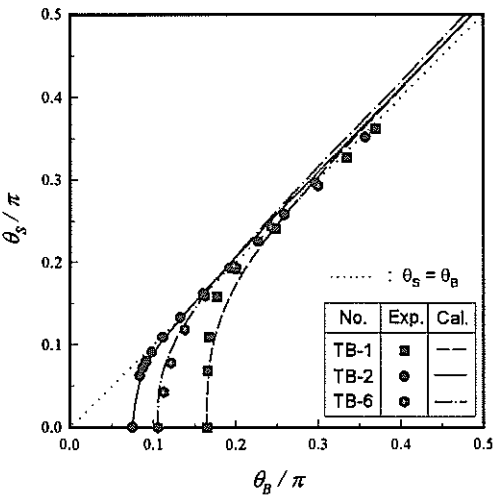

Fig.7 Correlation between the normalized outer half crack angle and the normalized inner half crack angle after penetration

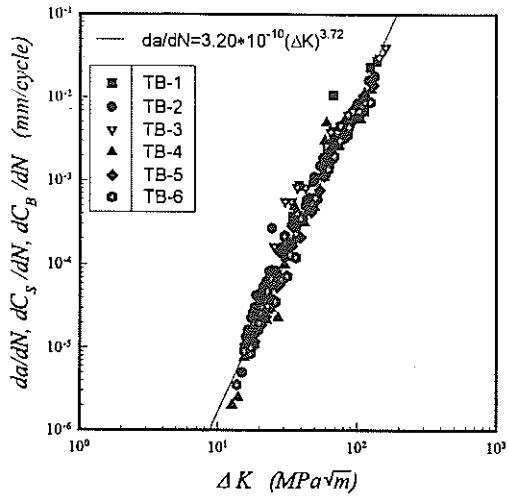

Fig.8 Fatigue crack growth rate versus stress intensity factor range

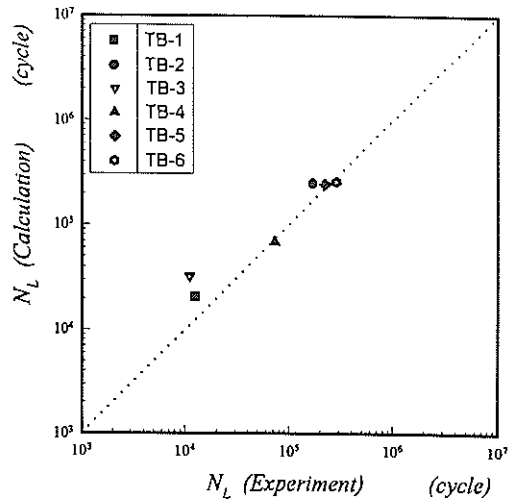

Fig.9 Comparison between the calculated and the experimental leak life

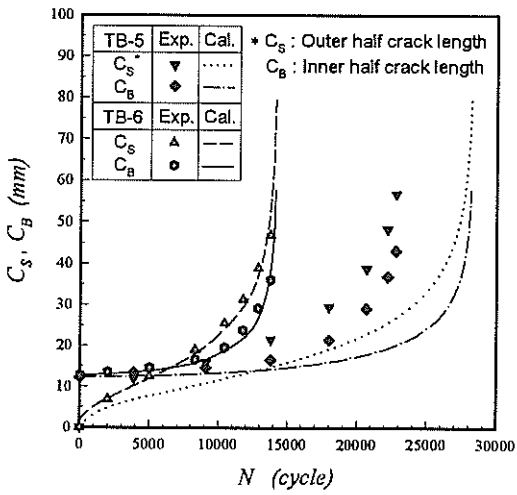

Fig.10 Comparison between the calculated and the experimental fatigue crack growth behavior after penetration

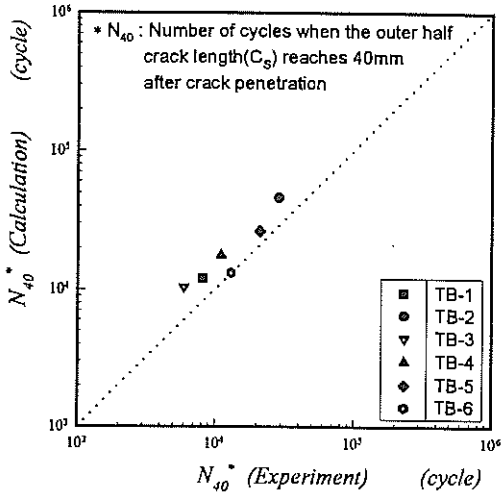

Fig.11 Comparison between the calculated and the experimental N_{40}